

Explaining the spectrum from the Galactic Centre using a two temperature plasma

Rohan Mahadevan

Institute of Astronomy, University of Cambridge, Madingley Road,
Cambridge, CB3 0HA, England

The radio source Sagittarius A* (Sgr A*), is thought to be a supermassive black hole located at the centre of our Galaxy,^{1,2} that is accreting gas from the surrounding region. Using the high inferred accretion rates,³ however, standard accretion models⁴ are unable to explain the low luminosity and observed spectrum from Sgr A*.^{5–8} A new accretion model has been proposed – an advection dominated accretion flow (ADAF),^{9–12} where most of the accretion energy is stored in the gas and lost into the black hole. The gas therefore has a two–temperature structure^{10,13,14} with the protons being much hotter than the electrons. The model explains the low luminosity from Sgr A*^{15–18} and most of the millimeter to hard X–ray spectrum, but has had serious difficulty in agreeing with the low energy radio observations.¹⁸ Here we report an emission process associated with the protons that naturally resolves the observed discrepancy. This provides, for the first time, observational evidence for a two–temperature plasma in hot accretion flows, and gives strong support to the idea that an ADAF does accrete onto a 2.5×10^6 solar mass black hole at the Galactic Centre.

Figure 1 shows the most up to date observations from the Galactic Centre.¹⁸ The spectrum rises at radio and sub–millimeter frequencies $\nu \sim 10^9 - 10^{12}$ Hz, where most of the emission occurs, and has a sharp drop in the infrared. The X–ray observations comprise of a possible detection at soft X–ray energies, and firm upper limits in the hard X–rays. The X–ray error–box corresponds to uncertainties in the observed photon index which lies between 1.0 and 2.0.¹⁸ At very high energies, EGRET has observed gamma–ray emission from the Galactic Center region.⁸ However, due to the low angular resolution of the measurements, $\sim 1^\circ$, the observations should perhaps be considered as upper limits.

The spectrum from a two–temperature ADAF is determined by the cooling properties of the protons and electrons in the flow. The protons are at virial temperatures at all radii ($T_p \sim 10^{12}$ K close to the black hole), and cool by creating neutral pions,¹⁹ while the electrons have much lower temperatures ($T_e \sim 10^{9.5}$ K) and cool by various optically thin processes, viz. synchrotron, inverse Compton and bremsstrahlung radiation.^{11,20}

Figure 1a shows the spectrum from the ADAF model of Sgr A* in ref. 18. The spectrum fits the sub–millimeter to hard X–ray spectrum quite well, but fails to explain the non–uniform radio spectrum. The radio spectral dependence is well represented by $L_\nu \propto \nu^{0.2}$ up to $\nu \sim 43$ GHz, which subsequently rises to $L_\nu \sim \nu^{0.8}$ for $\nu \gtrsim 86$ GHz.²¹

ADAF models of Sgr A* have always been unable to account for this break, and are substantially underluminous at frequencies below ~ 86 GHz. This poses a serious problem.

The observed excess of radio emission (beyond what the model predicts) has usually been attributed to a weak jet of material that might emerge from the ADAF; jets are known to be strong radio sources. High resolution radio observations, however, have ruled this out,^{22–24} which severely constrains any outflow models. In this case a rather ad hoc electron temperature profile might be needed to account for the excess radio emission,¹⁸ which is probably unphysical. More importantly, recent high resolution measurements constrain the actual size of the emitting region.^{5,22} These observations require large brightness temperatures in excess of 10^{10} K to explain the observed flux at 43 GHz and 86 GHz. In an ADAF, however, the electron temperatures are always well below 10^{10} K at all radii,¹¹ and therefore cannot account for these high temperatures.

This apparent problem is solved by considering another emission process associated with the protons. In addition to producing neutral pions, energetic proton collisions can also create charged pions which subsequently decay into positrons and electrons (e^\pm). This had been neglected in earlier work since these particles do not produce significant amounts of gamma-ray emission.¹⁹

The high energy e^\pm , however, can interact with the magnetic fields in the ADAF to produce synchrotron emission from radio to hard X-ray energies. Since the pions, and therefore the e^\pm , are created by proton–proton collisions, the energy spectra of the protons and e^\pm are related. This allows a direct investigation of the assumption that the protons have a different average temperature than the electrons, and at the same time determines if the e^\pm are created in sufficient number, and with the right energy, to produce the observed radio emission.

For the present discussion, we assume that the energy spectrum of the protons is represented by a power-law distribution, $N(E_p) \propto E_p^{-s}$ with index s . The index is generally between 2 and 4, and we set it to $s = 2.75$, at the cosmic ray value, suggesting that a similar acceleration mechanism might be at work in ADAFs.¹⁹ The results are insensitive to the exact value of s .¹⁹

The rate of production and energy spectrum of the e^\pm , $R(E)$, is determined by the frequency of proton collisions as well as their energy spectrum. For the assumed power-law proton distribution, the energy distribution of the e^\pm is shown in Figure 2. The spectrum rises at low energies, turns over at $E \sim 35$ MeV, and, as expected, extends as a power-law, E^{-s} , with the same energy dependence as the parent proton distribution.²⁵ Since the created charged pion has a mass of ~ 140 MeV and decays into four particles, one of which is an electron or positron, we expect that on average the e^\pm should carry away one fourth of the total energy available $\sim 140/4 = 35$ MeV.²⁶ This is an expected turnover which is characteristic of e^\pm production, and is shown in Figure 2.

Determining the synchrotron emissivity from the e^\pm , requires a knowledge of their

steady state energy distribution $N(E)$. At a given energy E , the colliding protons produce $R(E)$ electrons and positrons. However, since the e^\pm cool by synchrotron radiation, they lose their energy very efficiently, and the steady state distribution is therefore determined by the competing effects of the creation and depletion of particles. This requires that the net flux of particles between two energies be equal to their rate of injection, $d[N(E) \dot{E}_S(E)]/dE = R(E)$, where $\dot{E}_S(E)$ is the total synchrotron cooling rate as a function of energy.²⁷

Using the steady state distribution $N(E)$, the e^\pm synchrotron spectrum, from the ADAF around Sgr A*, is shown by the dotted line in Figure 1b. The spectrum rises at low frequencies, turns over, and extends as a power-law at high frequencies. The spectral break at $\nu \sim 10^{15}$ Hz is a direct consequence of the turn over in the e^\pm energy spectrum shown in Figure 2. At high frequencies, the spectrum is optically thin and has a spectral dependence $L_\nu \propto \nu^{-s/2}$. The spectral slope therefore depends on the proton index s , which is a direct consequence of the e^\pm having a steady state distribution $N(E) \propto E^{-(s+1)}$.²⁷ At lower frequencies, the expected optically thin spectral dependence is $L_\nu \propto \nu^{-0.5}$ which corresponds to $N(E) \propto E^{-2}$.²⁷ However, in an ADAF, the emission at these low frequencies is self-absorbed by the plasma and the resultant spectrum shown therefore has a different spectral dependence.

The solid curve in Figure 1b represents the total radiation from the ADAF which includes this spectrum. At high frequencies $\gtrsim 10^{13}$ Hz, the synchrotron emission contributes to, but does not significantly change the total luminosity. In particular the agreement with the X-ray flux is not affected, and the additional infrared flux is still well below the stringent upper limits.

At lower energies the result is striking. The emission reproduces the required spectral break at ~ 86 GHz, is able to account for the “excess” radio emission below this frequency, and diminishes sufficiently quickly at lower frequencies to agree with the radio upper limit at 400 MHz. Since the emission at each radio frequency in Figure 1a corresponds to a black body spectrum at a given radius,^{11,20} the total spectrum shown by the solid line in Figure 1b indicates that ADAFs produce more emission at a given frequency than the local black body spectrum. The excess emission is from the high energy electrons radiating at larger radii. This resolves the problem with the low energy radio emission completely. No outflow model is needed to account for the observed emission, and the high brightness temperatures inferred^{5,22} are easily accounted for by the non-thermal origin of the emission.

The quite good agreement with the radio observations, suggests that the emission observed is most probably from the hot protons in the ADAF. However, before drawing any conclusions, it is interesting to examine the essential ingredients required to explain the radio spectrum. Assuming that the dynamics of the flow are determined, reproducing the radio spectrum requires high energy electrons (or e^\pm) with energies ~ 100 MeV at all radii. In an ADAF, this requirement is naturally satisfied. Assuming that viscosity

primarily heats the protons into a power-law distribution at all radii, the production of high energy e^\pm with the same energy is completely determined by only the nuclear physics of particle collisions and decays.^{25,26} In particular, the shape of the e^\pm spectrum (cf. Figure 2) is fixed throughout the flow. It is interesting that the number of e^\pm produced is also in the right amount; a natural consequence of the proton collision time being longer than the accretion time. While shorter collision times would produce excessive amounts of e^\pm which would result in too much radio emission, much longer collision times would result in too little radio emission.

The agreement of the theory with the observations depends on two basic assumptions of ADAFs that have always been debated: (1) the existence of a two temperature plasma, and (2) that viscosity preferentially heats the protons. It is interesting that for the first time, we have quite good observational evidence that the first assumption is probably true. This is because the radio to hard X-ray spectrum is determined by emission processes associated with both the protons and electrons, at their respective temperatures. If the temperatures were the same or markedly different from their calculated values, the resulting spectrum would be completely different and fail to explain any of the observations.

The second assumption is supported by the present results, and can be discussed in terms of δ , which is the fraction of viscous energy that heats the electrons. The baseline model in ref. 18 set $\delta \simeq 0.001$, and showed that for $\delta > 0.01$, too much radiation is produced, and the electron spectrum does not agree with the observations. Here, for the first time, we have a radiation mechanism that accounts for the other fraction $(1 - \delta)$ that heats the protons, and have shown that the agreement with the low energy radio spectrum requires the amount of energy transferred to the electrons to be small. This shows, for the first time, that the average energy of the protons is most likely virial.

While past work has attempted to answer both these questions theoretically,^{28–33} the results here provide indirect observational evidence that these assumptions are probably valid. Further, theoretical models which reach contrary conclusions are probably based on assumptions that are not valid in ADAFs.^{18,34} The present results could therefore be used as tools to aid future theoretical work in resolving these complex questions in plasma physics.

The present results have assumed that all the viscous energy is deposited into a power-law proton distribution, which might seem improbable. However, if half the viscous energy were transferred into a power-law distribution, and half into a thermal one, the number of e^\pm created reduces only by a factor ~ 2 ,¹⁹ and the results presented here do not change significantly. Therefore, while the agreement with the radio flux requires a power-law proton distribution, it does not require all of the viscous energy to be deposited into the power-law protons.

It is interesting that the good agreement with observations comes from a model in

which both the viscous hydrodynamics and radiative processes have been included self-consistently. Previous models that have attempted to explain the observed spectrum have either been phenomenological^{35–37}, made simplifying assumptions, such as ignoring the angular momentum of the accreting gas^{3,38,39}, or, as noted previously,^{18,40} have errors in the synchrotron calculation which renders the resulting spectrum suspect.^{3,39} The ADAF models therefore provides us with a unique self-consistent framework which enables accurate prediction of spectra from accreting black holes.

We stress that there is no fine tuning in the present results. While previous work on ADAFs has not included the e^\pm synchrotron radiation, the results presented here show that this process is essential to explaining the observed non-uniform radio spectrum. The model used is identical to that presented in ref. 18, and we have simply taken into account an additional physical process and emission mechanism in the two-temperature ADAF. It is quite remarkable that using the same parameters as in ref. 18, an emission mechanism associated with the protons is able to naturally reproduce the entire radio spectrum including the observed spectral break at ~ 86 GHz. The agreement of the theory with the observations, encourages us to take the natural explanation and conclude that Sgr A* is in fact a 2×10^6 solar mass black hole that is accreting via a two-temperature ADAF.

References:

1. Mezger, P. G., Duschl, W. J., & Zylka, R., The Galactic Center: a laboratory for AGN?. *ARA&A*, **7**, 289–388 (1996)
2. Genzel, R., Hollenbach, D., & Townes, C. H., The nucleus of our Galaxy. *Rep. Prog. Phys.*, **57**, 417–479 (1994)
3. Melia, F., An accreting black hole model for Sagittarius A*. *Astrophys. J.*, **387**, L25–L28 (1992)
4. Frank, J., King, A., & Raine, D., *Accretion power in astrophysics*. (Cambridge Univ. Press 1992)
5. Rogers, A. E. E., *et al.*, Small-scale structure and position of Sagittarius A* from VLBI at 3 millimeter wavelength. *Astrophys. J.*, **434**, L59–L62 (1994)
6. Menten, K. M., Reid, M. J., Eckart, A., & Genzel, R., The position of Sagittarius A*: accurate alignment of the radio and infrared reference frames at the Galactic Center. *Astrophys. J.*, **475**, L111–L114 (1997)
7. Predehl, P., & Trümper, J., ROSAT observation of the Sgr A region. *Astr. Astrophys.*, **290**, L29–L32 (1994)
8. Merck, M., *et al.*, 1996, Study of the spectral characteristics of unidentified galactic EGRET sources. Are they pulsar-like? *Astr. Astrophys. Supp.*, **120**, 465–469 (1996)
9. Ichimaru, S., Bimodal behavior of accretion disks - Theory and application to Cygnus X-1 transitions. *Astrophys. J.*, **214**, 840–855 (1977)
10. Rees, M. J., Begelman, M. C., Blandford, R. D., & Phinney, E. S., Ion supported tori and the origin of radio jets. *Nature*, **295**, 17–21 (1982)
11. Narayan, R., & Yi, I., Advection-dominated accretion: underfed black holes and neutron stars. *Astrophys. J.*, **452**, 710–735 (1995)
12. Abramowicz, M. A., Chen, X., Kato, S., Lasota, J.-P., & Regev, O., Thermal equilibria of accretion disks. *Astrophys. J.*, **438** L37–L39 (1995)
13. Shapiro, S. L., Lightman, A. P., & Eardley, D. M., A two-temperature accretion disk model for Cygnus X-1 - Structure and spectrum. *Astrophys. J.*, **204**, 187–199 (1976)
14. Phinney, E. S., Ion pressure-supported accretion tori and the origin of radio jets. A plea for specific advice on the plasma physics. in *Plasma Astrophysics* (ed. T. D. Guyenne & G. Levy). 337–341 (ESA SP-161, Paris, 1981)
15. Rees, M. J., The compact source at the Galactic Center. in *The Galactic Center* (ed. G. R. Riegler & R. D. Blandford). AIP, 166–176. (New York: 1982)
16. Narayan, R., Yi, I., & Mahadevan, R., Explaining the spectrum of Sagittarius A* with a model of an accreting black hole. *Nature*, **374**, 623–625 (1995)
17. Manmoto, T., Mineshige, S., & Kusunose, M., Spectrum of Optically Thin Advection-dominated Accretion Flow around a Black Hole: Application to Sagittarius A*. *Astrophys. J.*, **489**, 791–803 (1997)
18. Narayan, R., Mahadevan, R., Grindlay, J. E., Popham, R. G., & Gammie, C., Advection-dominated accretion model of Sagittarius A*: evidence for a black hole at the Galactic Center. *Astrophys. J.*, **492**, 554–568 (1998)
19. Mahadevan, R., Narayan, R., & Krolik, J., Gamma-ray emission from advection-

- dominated accretion flows around black holes: application to the Galactic Center. *Astrophys. J.*, **486**, 268–275 (1997)
20. Mahadevan, R., Scaling laws for advection–dominated flows: applications to low–luminosity galactic nuclei. *Astrophys. J.*, **477**, 585–601 (1997)
21. Falcke, H., *et al.*, The simultaneous spectrum of Sgr A* from $\lambda 20$ cm to $\lambda 1$ mm and the nature of the mm–excess. *Astrophys. J.*, **499**, in press (1998)
22. Backer, D. C., *et al.*, Upper limit of 3.3 astronomical units to the diameter of the Galactic Center radio source Sgr A*. *Science*, **262**, 1414–1416 (1993)
23. Marcaide, J. M., *et al.*, Position on morphology of the compact non–thermal radio source at the galactic center. *Astr. Astrophys.*, **258**, 295–301 (1992)
24. Alberdi, A., *et al.*, VLBA image of Sgr A* at $\lambda = 1.35$ cm. *Astr. Astrophys.*, **277**, L1–L4 (1993)
25. Ginzburg, V. L., & Syrovatskii, S. I., *The Origin of Cosmic Rays* (New York: Macmillan 1964)
26. Dermer, C. D., Binary collision rates of relativistic thermal plasmas. II. Spectra. *Astrophys. J.*, **307**, 47–59 (1986)
27. Rybicki, G., & Lightman, A., *Radiative Processes in Astrophysics* (New York: Wiley 1979)
28. Begelman, M. C., & Chiueh, T., Thermal coupling of ions and electrons by collective effects in two–temperature accretion flows. *Astrophys. J.*, **332**, 872–890 (1988)
29. Quataert, E., Particle heating by Alfvénic turbulence in hot accretion flows. *Astrophys. J.*, in press (astro-ph/9710127) (1998)
30. Gruzinov, A., Radiative efficiency of collisionless accretion. *Astrophys. J.*, in press (astro-ph/9710132) (1998)
31. Blackman, E., Fermi energization in magnetized astrophysical flows. *Phys. Rev. Lett.*, in press (astro-ph/9710137) (1998)
32. Bisnovatyi-Kogan, G.S. & Lovelace, R. V. E., Influence of Ohmic heating on Advection-dominated accretion flows. *Astrophys. J.*, **486**, L43–L46 (1997)
33. Quataert, E. & Gruzinov, A., Turbulence and particle heating in advection-dominated accretion flows. *Astrophys. J.*, submitted (astro-ph/9803112) (1998)
34. Narayan, R., Mahadevan, R., & Quataert, E., Advection–dominated accretion around black holes. in *The Theory of Black Hole Accretion Discs* (eds. M. A. Abramowicz, G. Bjornsson, & J. E. Pringle), in press (Cambridge Univ. Press 1998)
35. Duschl, W. J., & Lesch, H., The spectrum of Sgr A* and its variability. *Astr. Astrophys.*, **286**, 431–436 (1994)
36. Falcke, H., What is Sgr A*? in *Unsolved problems in the Milky Way* (ed. L. Blitz & P. J. Teuben). 163–170. (IAU Symp. No. 169, Kluwer, Dordrecht, 1996)
37. Beckert, T., & Duschl, W. J., Synchrotron radiation from quasi-monoenergetic electrons. Modeling the spectrum of Sgr A*. *Astr. Astrophys.*, **328**, 95–106 (1997)
38. Mastichiadis, A., & Ozeroy, L. M., X-ray and gamma-ray emission of Sagittarius A* as a wind-accreting black hole. *Astr. Astrophys.*, **426**, 599–603 (1994)
39. Melia, F., An accreting black hole model for Sagittarius A*. 2: A detailed study.

Astrophys. J., **426**, 577–585 (1994)

40. Mahadevan, R., Narayan, R., & Yi, I., Harmony in electrons: cyclotron and synchrotron emission by thermal electrons in a magnetic field. *Astrophys. J.*, **465**, 327–337 (1996)

41. Shakura, N. I., & Sunyaev, R. A., Black holes in binary systems. Observational appearance. *Astr. Astrophys.*, **24**, 337–355 (1973)

42. Haller, J., *et al.*, Stellar kinematics and the black hole in the Galactic Center. *Astrophys. J.* **456**, 194–205 (see also ERRATUM: *Astrophys. J.*, **468**, 955) (1996)

43. Eckart, A., & Genzel, R., Stellar proper motions in the central 0.1 pc of the Galaxy. *Mon. Not. R. Astr. Soc.* , **284**, 576–598 (1997)

Acknowledgments: I would like to thank R. Narayan, E. Blackman, A. Fabian, C. Gammie, Z. Haiman, J. Herrnstein, J. Krolik, A. Mody, M. Rees, and E. Quataert for discussions and comments.

Figure Captions:

Figure 1a:

The spectrum of Sgr A*: The horizontal axis is the log of the frequency and the vertical axis is the log of the energy at that frequency. The measured fluxes were converted to luminosities assuming a distance of 8.5 kpc to the Galactic Centre. The data are the most up to date compilation of observations taken from ref. 18. The arrows represent upper limits, and the box at frequency $\sim 10^{17}$ Hz represents the uncertainty in the observed photon index. The solid line is the spectrum from the baseline ADAF model of Sgr A* used in ref. 18. The ADAF parameters are $\alpha = 0.3$, $\beta = 0.5$, $M = 2.5 \times 10^6 M_\odot$, and $\dot{M} = 7.2 \times 10^{-6} M_\odot/\text{yr}$. Here, α is the viscosity parameter⁴¹, β determines the strength of the magnetic field, and is defined so that $(1 - \beta)$ is the ratio of magnetic to total pressure, M is the dynamically measured mass of Sgr A*^{42,43}, and \dot{M} is the mass accretion rate. For frequencies $\lesssim 10^{20}$ Hz, the spectrum is determined by the individual optically thin cooling processes of $\sim 10^{9.5}$ K thermal electrons, while for $\nu \gtrsim 10^{20}$ Hz the spectrum is solely due to the decay of neutral pions. The discrepancy of the model to the observations above $\nu \sim 10^{20}$ Hz is not considered serious since it is unclear at this time whether the $\sim 1^\circ$ beam of EGRET is detecting a point source or some diffuse emission. These observations should therefore be considered as upper limits rather than detections of a central source.

Figure 1b:

The solid line represents the total spectrum from the ADAF around Sgr A*, which includes the present results. The parameters used are identical to Figure 1a. The dotted line represents only the synchrotron emission from the e^\pm .

Figure 2:

The energy spectrum, $R(E)$, of e^\pm that are created by colliding power-law protons with energy index $s = 2.75$. The vertical axis is the log of number of e^\pm created per unit volume, per second, per energy interval, and the horizontal axis is the log of the energy. The scale on the vertical axis corresponds to a number density of protons equal to unity. For a number density N , the vertical axis must be multiplied by N^2 . The particles that are responsible for most of the emission are determined by the energy at which the function $E^2 R(E)$ peaks, which occurs between $100 \text{ MeV} < E < 500 \text{ MeV}$. The shape of the spectrum depends only on the physics of particle collisions and decays,^{25,26} and at high energies has the spectral shape $R(E) \propto E^{-s}$.²⁵ The spectrum therefore contains spectral information of the parent proton distribution, as well as determines the shape of the resulting synchrotron spectrum. It therefore acts as a link between the form of the proton energy distribution and the observed synchrotron spectrum.

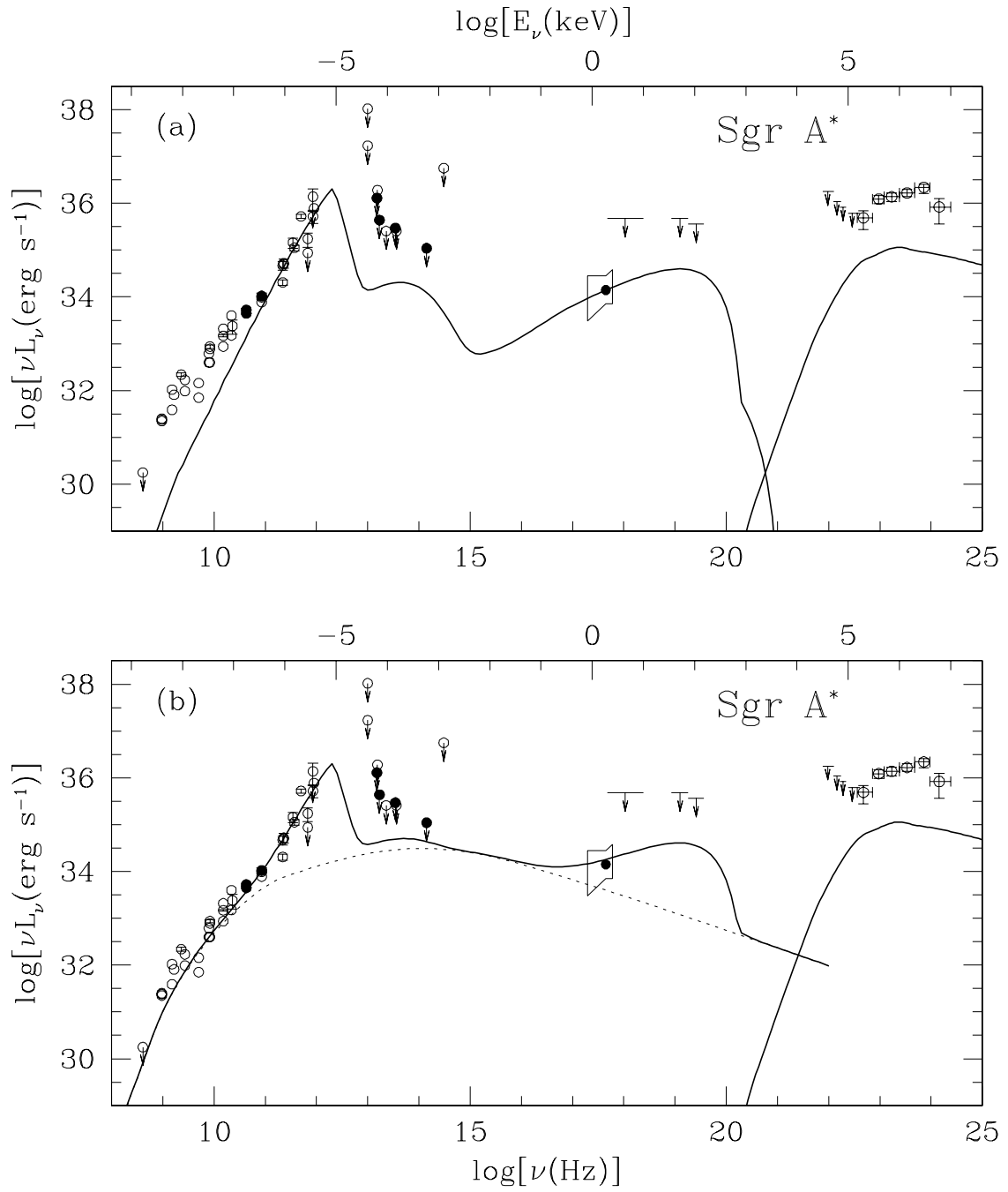


Figure 1

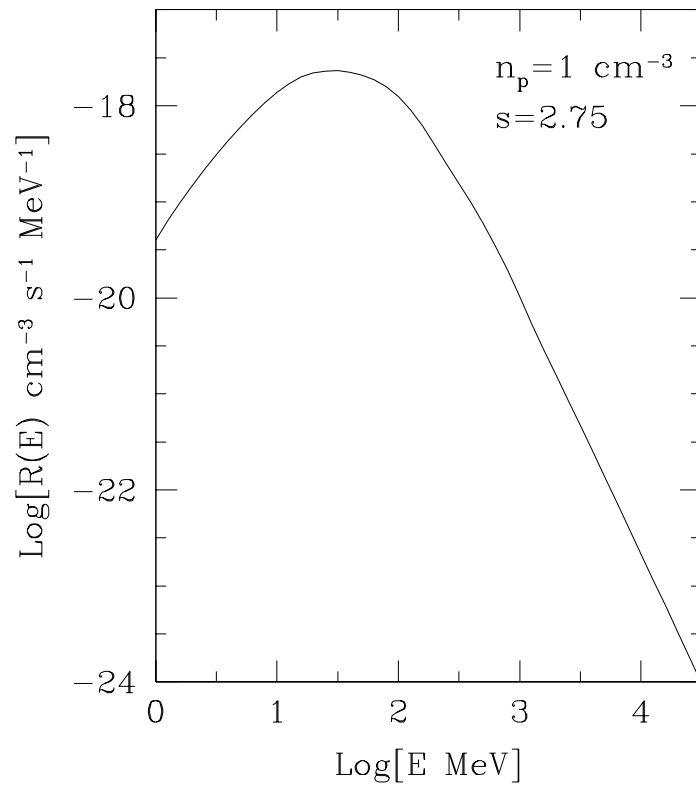


Figure 2